Investigation of the effect of thermal cycling on the device performance of $YBa_2Cu_3O_{7-\delta}$ DC-SQUIDs

IOP Publishing Superconductor Science and Technology
Supercond. Sci. Technol. **20** (2007) 944–949 doi:10.1088/0953-2048/20/10/008

Investigation of the effect of thermal cycling on the device performance of $YBa_2Cu_3O_{7-\delta}$ DC-SQUIDs

I Avci[1,2,5], B P Algul[1], A Bozbey[3], R Akram[4], M Tepe[2] and D Abukay[1]

[1] Physics Department, Izmir Institute of Technology, 35436-Urla, Izmir, Turkey
[2] Physics Department, Ege University, 35100 Bornova, Izmir, Turkey
[3] Electrical-Electronics Engineering, Bilkent University, 06800 Bilkent, Ankara, Turkey
[4] Department of Physics, Bilkent University, 06800 Bilkent, Ankara, Turkey

E-mail: ilbeyiavci@iyte.edu.tr

Received 16 May 2007, in final form 17 July 2007
Published 22 August 2007
Online at stacks.iop.org/SUST/20/944

Abstract
We investigated the effect of thermal cycling on the operational performance of $YBa_2Cu_3O_{7-\delta}$ (YBCO) direct current superconducting quantum interference devices (DC-SQUIDs) fabricated onto 24° $SrTiO_3$ (STO) bicrystal substrates. The devices under investigation consist of directly coupled DC-SQUID magnetometer configurations. Thin films having 200 nm thicknesses were deposited by dc-magnetron sputtering and device patterns were made by a standard lithography process and chemical etching. The SQUIDs having 4 μm-wide grain boundary Josephson junctions (GBJJs) were characterized by means of critical currents, peak-to-peak output voltages and noise levels, depending on the thermal cycles. In order to achieve a protective layer for the junctions against the undesired effects of thermal cycles and ambient atmosphere during the room temperature storage, the devices were coated with a 400 nm thick YBCO layer at room temperature. Since the second layer of amorphous YBCO is completely electrically insulating, it does not affect the operation of the junctions and pick-up coils of magnetometers. This two-layered configuration ensures the protection of the junctions from ambient atmosphere as well as from the effect of water molecules interacting with the film structure during each thermal cycle.

1. Introduction

In superconducting electronics, a number of applications based on SQUIDs require an optimized Josephson junction technology for successful operations. Such an appropriate technology should yield the junctions with controllable and reproducible parameters including non-hysteretic resistively shunted junction (RSJ) type I–V characteristics [1, 2], high I_cR_n product, low levels of $1/f$ noise [3], high stability under room temperature storage and non-degradable parameters during thermal cycling. Although these requirements have been well satisfied in low-T_c junctions by niobium technology [4], the development of such a successful technology in high-T_c SQUIDs with YBCO thin films have been the major challenge. Despite this fact, there have been many studies on YBCO junctions ranging from single layer to multilayer such as bicrystal, step-edge, ramp-edge and superconductor–normal metal–superconductor type junctions [5, 6] and [7]. Furthermore, the most successful results have been obtained from grain boundary Josephson junctions (GBJJs) fabricated on top of the grain boundary of bicrystal substrates, which have a relatively easier fabrication process yielding highly reproducible parameters; hence, bicrystal GBJJs have been the preferred technology in SQUID

[5] Address for correspondence: Physics Department, Izmir Institute of Technology, 35436-Urla, Izmir, Turkey.

fabrication [8]. However, it is fair to say that an appropriate technology for high-T_c junctions has not yet been established for obtaining similar successful results compared to the low-T_c counterparts. The main reason underlying this fact is related to the fabrication complexity of good quality high-T_c junctions, which requires a large amount of strong pinning sites in the *c*-axis direction and high critical current density in the *ab* plane, depending on the crystalline structure of YBCO thin films and low noise caused by the thermal fluctuations [9, 10].

Another reason is the difficulty of maintaining the stability of SQUIDs for a long time during their storage at room temperature and their durability against thermal cycles which will be considered throughout this study. Besides the complexity of the crystalline structure, the chemical structure of YBCO is highly sensitive to moisture [11]. The interaction of water with YBCO thin films gives rise to a degradation of superconducting properties which hinders the functioning of devices at optimal conditions. The Josephson junctions made of YBCO thin films are inevitably introduced to water during lithographic and chemical etching processes. Additionally, during each thermal cycling, the device is exposed to moisture and water vapor condensed on it in a short time. All those factors cause a considerable reduction in the device performance. The studies [12, 13] in the literature and references therein have been devoted to explore the mechanism of interactions between YBCO and water molecules, giving possible solutions for the recovery of superconductivity. In our study, we investigated the influences of such undesired effects on the device performance of DC-SQUIDs caused by thermal cycles and possible solutions to maintain the long time stability of them by using a protective layer made of room-temperature-deposited YBCO thin films (amorphous α-layer) over the junctions.

2. Experimental procedure

The method in this study is based on the room temperature deposition of a protective YBCO layer on top of the DC-SQUIDs. We used two different DC-SQUIDs; one without a protective layer and a second with an amorphous YBCO protective layer. 200 nm thick YBCO thin films were deposited by DC magnetron sputtering onto 24° (100) bicrystal STO substrates. The devices under investigation consist of directly coupled DC-SQUID magnetometer configurations which have 4 μm wide grain boundary Josephson junctions patterned by standard lithography and wet etching processes. The outer dimensions of the magnetometers were chosen as 9 mm × 9 mm leaving narrow edges on 10 mm × 10 mm STO substrates to decrease the edge effects and increase the effective area of the pick-up loop. The pick-up loop includes a square hole with one edge of 3 mm placed at the center. The SQUIDs were designed to have a total SQUID loop inductance of $L_s \approx 67$ pH, pick-up loop inductance of $L_p \approx 4.7$ nH, pick-up loop area of $A_p \approx 27$ mm^2 and effective area of $A_{eff} \approx 0.31$ mm^2. The total SQUID inductance including the parasitic inductance of junction striplines was calculated by using the coplanar strip line approximation [14]. The design parameters are given in table 1.

In order to have a protecting layer over the junctions, the devices were coated with a 400 nm thick YBCO layer at room temperature. Since the second layer YBCO is completely electrically insulating, it has no effect on the operation of the junctions and magnetometer's pick-up coils. This two-layered configuration ensures the protection of the junctions from the ambient atmosphere as well as from the effect of water molecules interacting with the film structure during each thermal cycle. The diagram of the fabrication process is given in figure 1.

Table 1. Design values for the directly coupled DC-SQUID magnetometer with a YBCO film thickness of 200 nm.

Parameter	Value
$L_{geo,junc}$	8 pH
$L_{kin,junc}$	5 pH
$L_{geo,wash}$	37 pH
$L_{kin,wash}$	17 pH
L_p	4.7 nH
A_p	27 mm^2
A_{eff}	0.31 mm^2

After making the SQUID, the room temperature amorphous YBCO thin film was deposited as a passivation layer on top of the SQUID by protecting the contact pads of the device with a shadow mask. Later a photoresist was spun on and a window was opened over the contact pads. Then, a 70 nm thin gold contact metallization has been done using a sputtering system. The gold layer, except at the contact pads, was removed by a lift-off step. This gold layer prevents the device electrodes from oxidation during long term storage. The chip was then placed into a chip carrier made by a printed circuit board (PCB) material having a printed feedback coil, and the electrical connections were made by a wedge bonder using gold wire.

In this study, we fabricated five different protected SQUIDs to ensure the usefulness of the amorphous YBCO protective layer and we observed similar behaviour in all samples with slight differences which might come from slight variation in the fabrication process. The SQUIDs were characterized by means of I–V, V–Φ and noise characteristics regarding the device performance in liquid nitrogen inside a magnetically shielded environment made of two-layer μ-metal. The measurements of both non-protected and protected devices were made during more than thirty thermal cycles and the results were obtained in three parts regarding the change in characteristics: for the first cycle just after the fabrication, after the fifteenth cycle and at the last thermal cycle. V–Φ characteristics of unprotected SQUIDs were further measured at different bias current performing the dependence of output voltage modulation versus applied bias current values depending on the thermal cycles. The measurements were done by directly dipping the SQUIDs into liquid nitrogen baths and after the measurements they were warmed up to room temperature by directly drying them with a simple hair-dryer for 1 min. The SQUIDs were stored in a device box in the cleanroom environment for 48 h between each thermal cycling. According to our measurement results, DC-SQUIDs with passivation layers showed very stable operation performance even after many thermal cycles, as explained in the following sections in detail.

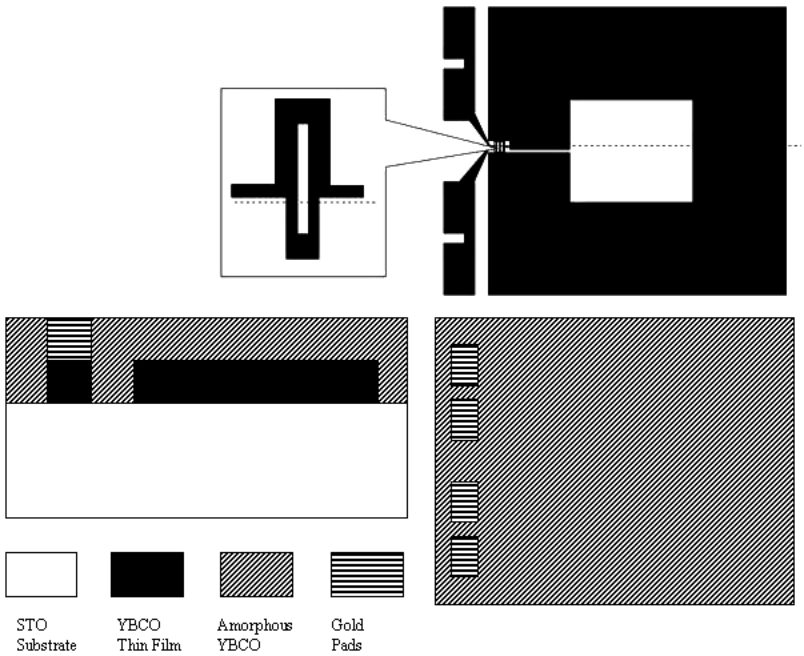

Figure 1. The layout of the DC-SQUID circuit and the step coverage of the fabrication process of DC-SQUIDs with an amorphous YBCO protecting layer.

3. Results and discussion

All of the measurements were made to investigate the effects of thermal cycling before and after the addition of a passivation layer for two different SQUIDs and results compare the devices' characteristics depending on the cycling effects. The current–voltage characteristics of the DC-SQUIDs were performed at 77 K under zero applied field in a magnetically shielded environment by directly dipping the SQUIDs into liquid nitrogen. After finalizing the fabrication optimization of the thin film deposition conditions and device fabrication process, I–V characteristics of SQUIDs at the first thermal cycle showed that the properties obtained were close to the predicted values of the RSJ model having the critical currents of $I_c = 32\ \mu$A and normal state resistance of $R_n = 2\ \Omega$ with the product of $I_c R_n \approx 65\ \mu$V. These values are typical for our DC-SQUIDs and small variations can be observed from device to device depending on the chemical etching process, yielding the small difference in junction widths. The peak-to-peak values of V–Φ characteristics of the SQUIDs also depend on the magnetometer configuration, design parameters and success of the lithography that should enable us to achieve the desired dimensions especially in the junction widths. Along with our process, we tried a number of fabrication processes, then we obtained those relatively high values of $I_c R_n$ and V_{pp} in the 4 μm junctions and we present those optimized values here.

Current–voltage characteristics of the DC-SQUID without a protective layer showed significant differences after a number of thermal cycles regarding the degradation of critical current values as shown in figure 2(a). We observed that both long term room temperature storage and a number of thermal cycles between liquid nitrogen and room temperature are significantly affecting the junctions. For example, the critical current of the device at 77 K that we report in this study decreased from 32 μA down to 2 μA and the normal state resistance, R_n, of the junctions increased up to 15 Ω at 77 K after approximately thirty cycles as shown in figure 2(a).

Though we report the experimental results of a pair of DC-SQUIDs here, we observed that the uniformity and surface morphologies of the thin films deposited on top of the grain boundary line of the substrates play important roles in the thermal cycle dependence of the I–V characteristics of the devices as expected. We saw that the different substrates purchased from different manufacturers showed different thermal cycle stability which mostly depends on the surface conditions of the substrates and the difference can be reach up to 30% or larger in the values of critical current and voltage modulation. Although the devices without protecting layers showed different dependences against the number of cycles and storage time, all of them have tended to reduce the critical current values as well as the output voltage in long term usage. On the other hand, the SQUIDs with a 400 nm thick amorphous YBCO layer deposited on top of them have almost maintained the critical current values as well as the shape of the I–V characteristics in that period of time including approximately thirty thermal cycles as seen in figures 2(a) and (b).

We could give some physical reasons for the decrease in I_c values depending on the thermal cycling process, as the widths of the Josephson junctions and the thin film are probably reduced by moisture due to the creation of a non-superconducting layer in the upper part of the film and at the edges of the junction striplines after many thermal cycles. Another reason may be the occurrence of micro-cracks through the junctions during the thermal cycling due to the stress between the thin film and the substrate in the grain boundary region. The last reason can be considered as the decrease in the

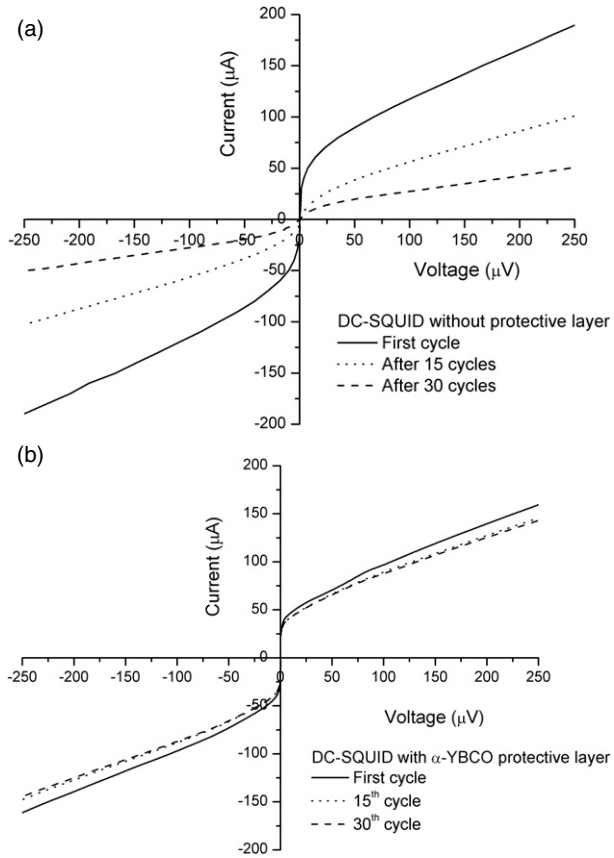

Figure 2. I–V characteristics of DC-SQUIDs at 77 K depending on the thermal cycles. (a) Unprotected DC-SQUID, (b) DC-SQUID with amorphous YBCO layer. Solid, dotted and dashed lines represent the measurements for the first, 15th and 30th thermal cycles, respectively.

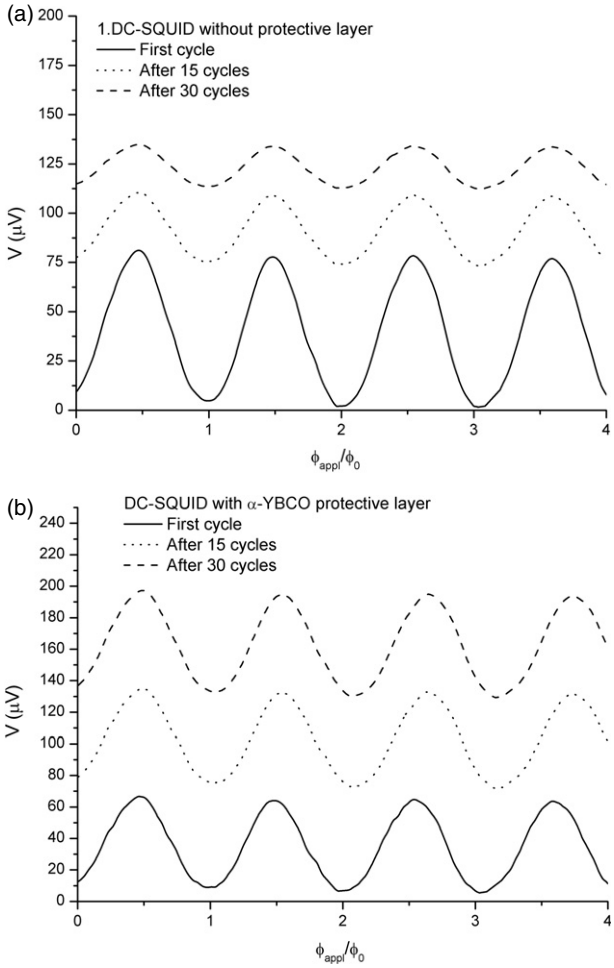

Figure 3. Output signals of the DC-SQUIDs depending on the thermal cycles. The curves are shifted vertically for clarity. (a) Unprotected DC-SQUID, (b) DC-SQUID with 400 nm thick amorphous YBCO layer. Solid, dotted and dashed lines represent the measurements for the first, 15th and 30th thermal cycles, respectively. The SQUIDs were modulated by a three-turn feedback coil by applying 20 Hz AC signal with 1.5 V_{pp}.

critical temperature of the upper part of the film and the edges of the junctions in which the superconducting properties were degraded by moisture.

The SQUID output signals are shown in figures 3(a) and (b) for both of the SQUIDs without and with an insulating YBCO layer, respectively. V–Φ measurements were made by flux-locked loop (FLL) electronics inside the μ-metal shield and the SQUIDs were modulated by a three-turn feedback coil, which was driven with a 20 Hz sawtooth waveform having the peak-to-peak amplitude of 1.5 V. In this configuration, we observed the voltage modulation of SQUIDs on the x–y mode of the oscilloscope. When a 1.5 V peak-to-peak amplitude of AC signal was applied to the feedback coil, it showed a countable amount of flux quanta as in figure 3. The maximum peak-to-peak voltage modulation (V_{pp}) of SQUID without the passivation layer was 65 μV with the bias current of 35 μA in the first thermal cycle.

Similar to the effect of the thermal cycle on the critical current, the peak-to-peak output voltage was also reduced to half of its original value after a number of thermal cycles and it tended to reduce further with increasing numbers of cycles. In our SQUIDs before putting the amorphous protective layer, some of the SQUIDs showed a degradation in their characteristics and continued working with very low critical currents as well as the output voltages. However, most of them stopped working because of the thermal influences. As seen from in figure 3(b), the voltage output value of an amorphous YBCO coated DC-SQUID did not change considerably during the course of this study.

The thermal cycle dependence of the SQUID output signal versus the bias current was also analyzed in this study. For all measurements during the thermal cycle procedure, the bias current dependences of V_{pp} showed similar behavior as all have a single peak with reduced current values as given in figure 4.

The peak-to-peak output voltages of non-protected SQUID showed characteristic bias current dependences during thermal cycles; that is, the voltages increase with the increasing bias currents up to certain values and start to decrease from maximum values when the bias currents further increase.

We also measured the noise characteristics of our DC-SQUIDs. The noise spectra of the devices were measured in the frequency bandwidth of 1 Hz–1 kHz by a spectrum analyzer directly connecting the SQUID electronics output to the analyzer input.

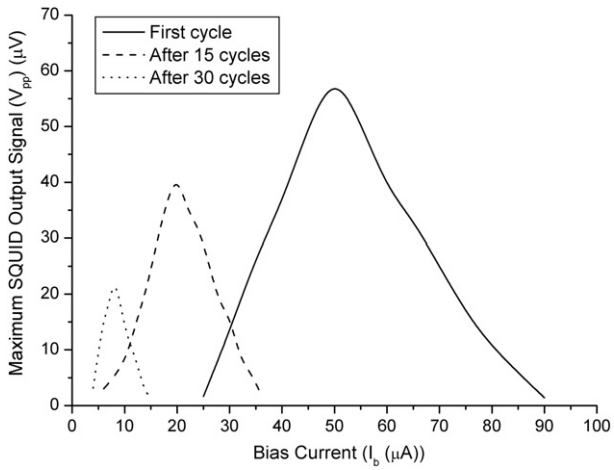

Figure 4. Bias current dependence of unprotected DC-SQUID output voltages during the thermal cycles. Bias current versus V_{pp} dependence showed a single peak in all measurements with reduced current values as well as the maximum peak-to-peak voltage values.

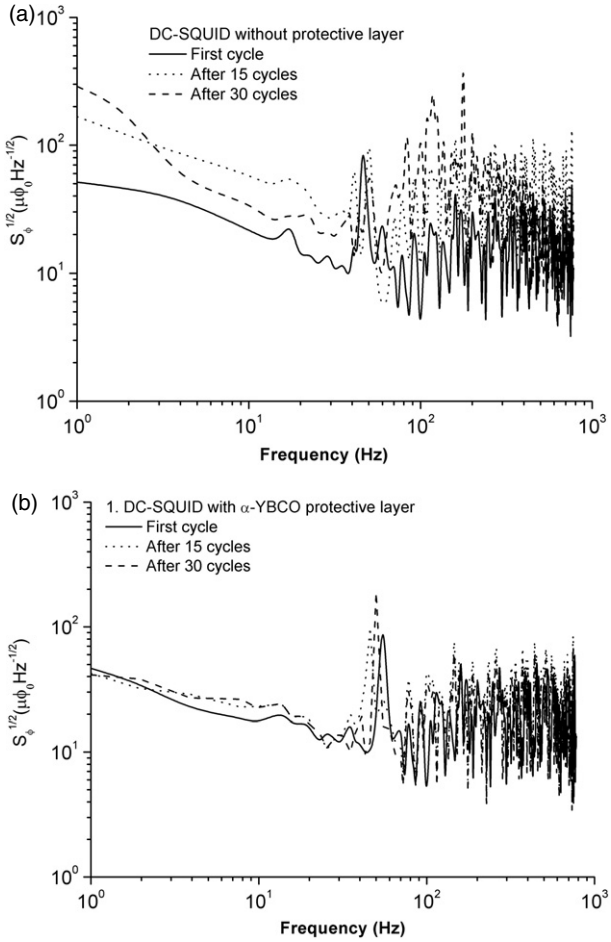

Figure 5. Noise spectrum of DC-SQUIDs showing flux noises with spectral power densities. (a) Unprotected DC-SQUID, (b) DC-SQUID with 400 nm thick amorphous YBCO layer. Solid, dotted and dashed lines represent the measurements for the first, 15th and 30th thermal cycles, respectively.

The noise characteristics were measured at bias currents which provide maximum peak-to-peak voltage modulation of SQUID output voltage using the low noise integrated flux-locked loop (FLL) electronics. The SQUID probe was immersed directly in the liquid nitrogen dewar placed in the cylindrical two-layer μ-metal shield. In the white noise regime, for the first cycle, the SQUID showed the flux noise with spectral power density of about 12 $\mu\phi_0$ Hz$^{-1/2}$ and field noise of about 38 fTHz$^{-1/2}$ at 1 kHz. The $1/f$ field noise was obtained as 145 fTHz$^{-1/2}$ at 1 Hz. As shown in figure 5(a), by increasing the number of thermal cycles for the unprotected SQUID, the noise picture of the device has also showed changes as in the output voltage and critical current. In the white noise regime, at the fifteenth thermal cycle, the device showed the field noise level of 161 fTHz$^{-1/2}$ at 1 kHz, and in the $1/f$ regime, it showed the field noise level of 580 fTHz$^{-1/2}$ at 1 Hz. These values tended to increase as the number of cycles increased. The reason for this noise picture can be expressed as the increase of the critical current fluctuations and the thermal noise current become more effective during the thermal cycles as the critical current reduces to very low values. The second reason may be considered that the junction and the SQUID loop structures are strongly affected by the ambient atmosphere in time. The water penetrates into the structure causing degradation there, hence weakening the pinning sites in the loop structure and creating a large amount of hopping of flux vortices in the SQUID loop and causing an excess noise contribution. As seen in figure 5(b), the protected SQUID with an amorphous YBCO layer has almost the same noise picture after a number of thermal cycles in the period of this study.

4. Conclusion

The stability problem of high-T_c SQUIDs is due to the external factors like moisture and stresses during thermal cycling which both cause considerable degradation of performance in long term use and storage of the devices. In order to keep the operational performance of the SQUIDs stable in time and during thermal cycles for long term usage, the method that we investigated shows that the passivation of the junctions as well as the magnetometer pick-up loop by depositing an amorphous layer of YBCO thin film at room temperature is an effective way. This second layer of YBCO thin film is fully insulating and does not have any effect on the operation of SQUID. Here, we have presented our results obtained from coating the Josephson junctions and associated magnetometer coils on the same chip by an amorphous YBCO second layer. Compared with the uncoated samples, this method created a considerable effect towards stabilizing the SQUIDs against thermal cycle effects as well as improving their storage time to longer periods without losing their initial optimal performances.

Acknowledgments

This study was supported by the TUBITAK with project nos. MISAG-264 and MAG-104M194.

References

[1] Stewart W C 1968 *Appl. Phys. Lett.* **12** 277
[2] McCumber D E 1968 *J. Appl. Phys.* **39** 3113

[3] Koelle D, Kleiner R, Ludwig F, Dantsker E and Clarke J 1999 *Rev. Mod. Phys.* **71** 644–78
[4] Gurvitch M, Washington M A and Huggins H A 1983 *Appl. Phys. Lett.* **42** 472
[5] Simon R *et al* 1991 *IEEE Trans. Magn.* **27** 3209
[6] Gao J, Aarnink W A M, Gerritsma G J and Rogalla H 1990 *Physica* C **171** 126
[7] DiIorio M S, Yoshizumi S, Yang K-Y, Zhang J and Maung M 1991 *Appl. Phys. Lett.* **58** 2552
[8] Hilgenkamp H and Mannhart J 2002 *Rev. Mod. Phys.* **74** 485–52
[9] Gross R, Chaudhari P, Kawasaki M, Ketchen M B and Gupta A 1990 *Appl. Phys. Lett.* **57** 727
[10] Gross R, Chaudhari P, Kawasaki M, Ketchen M B and Gupta A 1990 *Physica* C **170** 315
[11] Yan M F, Barns R L, O'Bryan H M Jr, Gallagher P K, Sherwood R C and Jin S 1987 *Appl. Phys. Lett.* **51** 532–4
[12] Rekhi S, Bhalla G L and Trigunayat G C 1998 *Physica* C **307** 51–60
[13] Bansal N P and Sandkuhl A L 1988 *Appl. Phys. Lett.* **52** 323–5
[14] Yoshida K, Hossain M S, Kisu T, Enpuku K and Yamafuji K 1992 *Japan. J. Appl. Phys.* **31** 3844–50